Studies of Double-Layer Effects at Single Crystal Gold Electrodes II. The Reduction Kinetics of Hexaaquairon(III) Ion in Aqueous Solutions

Magdalena Hromadová and W. Ronald Fawcett*

Department of Chemistry, UC Davis, California 95616

Received: June 27, 2000; In Final Form: September 25, 2000

The reduction kinetics of hexaaquairon(III) was studied at different concentrations of perchloric acid at four single-crystal gold electrodes. The electron-transfer rate constants obtained at constant electrode potential increase in the following order: Au(210) < Au(110) < Au(100) < Au(111). The experimental transfer coefficients increase in the same order. An analysis of double-layer effects within the framework of the classical Frumkin approach was consistent with the transport of a reactant of charge 2+ through the double-layer region and gave a value of the apparent transfer coefficient α_a equal to 0.3 for all single-crystal electrodes studied. The α_a value was rationalized by the distribution of charges within the reactant and product. The differences between double-layer effects on the reduction kinetics of hexaaquairon(III) and hexaamminecobalt-(III) ions are discussed.

Introduction

In a previous paper,[1] the importance of double-layer studies in connection with the measurement of electron-transfer kinetics at different single-crystal electrodes was emphasized. It was found that the kinetics of reduction of $Co(NH_3)_6^{3+}$ ion at four single-crystal electrodes, measured at a constant value of the applied potential, increase in the following order: Au(210) < Au(110) < Au(100) < Au(111). However, after correction for double-layer effects, the kinetic data fall on one linear plot for all single crystals and a single value of the apparent transfer coefficient is obtained for this electrode reaction. On the other hand, the double-layer corrected rate constants still depend on some characteristic properties of the electrode and the redox species, such as the potential of zero charge or the work function of the single crystal, and its relation to the standard potential of the $Co(NH_3)_6^{3+/2+}$ couple.

In this paper, attention is focused on the reduction of the $Fe(H_2O)_6^{3+}$ cation. Both, $Co(NH_3)_6^{3+}$ and $Fe(H_2O)_6^{3+}$ ion are reduced through an outer-sphere electron-transfer process, but electron transfer in the case of $Fe(H_2O)_6^{3+}$ cation is considered to be diabatic.[2−4] Both reactants are octahedral complexes, but the distribution of charges within the $Fe(H_2O)_6^{3+}$ ion is different from that of $Co(NH_3)_6^{3+}$ ion studied earlier.[5,6] This fact prompted us to investigate the ferric ion system in greater detail, since the high value of the apparent transfer coefficient for the reduction of $Co(NH_3)_6^{3+}$ ion can be attributed to the distribution of charge within the reactant and product, rather than to other features of the electron-transfer process.[1]

Electron transfer in the ferric/ferrous system has been extensively studied from a theoretical point of view.[2,3,4,7−19] Rose and Benjamin[14] used molecular dynamics to calculate the rate of electron transfer as a function of overvoltage for $Fe(H_2O)_6^{3+}$ ion reduction at the Pt-water interface. The calculations yielded a value of the activation energy at zero overvoltage equal to 58 ± 4 kJ mol^{-1}. This compares well with the experimental result of 56.8 ± 0.4 kJ mol^{-1} reported by Curtiss et al.[4] which was estimated assuming that the major contribution to the activation energy is solvent reorganization. Smith and Halley[3] calculated the activation energy to be in the range 51−68 kJ mol^{-1} and showed that the reduction of $Fe(H_2O)_6^{3+}$ ion can change from an adiabatic to a diabatic outer-sphere process at around 400 pm from the metal surface. However, a significant reduction rate during the process of simulation was observed only at distances larger than 500 pm, confirming the diabaticity of this reduction process. Curtiss et al.[4] arrived at a similar conclusion in their ab initio calculations.

In many of these theoretical studies, the $Fe(H_2O)_6^{3+}$ ion was assumed to have an octahedral geometry with Fe−O distances of 200−205 pm, and the Fe−H distance equal to 281 pm.[6,10,13,20] Neutron scattering experiments gave 201 pm for the Fe−O distance in concentrated electrolyte solutions.[21] The most reliable experimental determination of the Fe−O distance (198 pm) was obtained by the EXAFS method[22] in aqueous solutions.

In early simulations[3,14,15] of the $Fe(H_2O)_6^{3+}$ ion, the charge on the central iron atom was assumed to be +3 with +0.41 on each hydrogen atom and −0.82 on each oxygen atom. However, on the basis of recent calculations by Nazmutdinov,[5] the charge on the iron atom in $Fe(H_2O)_6^{3+}$ ion is +2.52, on the oxygen atom, −1.10, and on the hydrogen atom, +0.59. These values are in good agreement with the calculations of Martin et al.,[6] who obtained values of +2.15, −1.02, and +0.58, respectively. Martin et al.[6] also calculated the charge distribution in the conjugate base of $[Fe(H_2O)_6]^{3+}$, namely, the $[Fe(H_2O)_5OH]^{2+}$ ion. In this case, the charge on the iron is +1.62, and the charges on oxygen and hydrogen atoms are less positive and negative than those in the $Fe(H_2O)_6^{3+}$ ion.

Electron transfer in the $Fe^{3+/2+}$ system has been studied at many substrates and experimentally observed values of the formal potential range from 0.74 to 0.77 V against the normal hydrogen electrode.[4,23−28] Curtiss et al.[4,23] reported an experimental transfer coefficient of 0.59 and a standard rate constant of 2.2×10^{-5} cm s^{-1} at a polycrystalline gold electrode in solutions carefully purified from chloride ions. The latter value is close to the result reported by Weber et al.[24] A slightly higher value of 17.6×10^{-5} cm s^{-1} was reported by Abdelaal et al.[25]

There are only a few studies that have used single-crystal gold electrodes as a substrate.[28−31] Samec[28] studied the reduction of $Fe(H_2O)_6^{3+}$ ion at a Au(110) electrode. Since the experi-

10.1021/jp002299d CCC: $20.00
Published on Web 12/12/2000

mentally observed transfer coefficients did not depend on the concentration of supporting electrolyte, the author concluded that the reaction site must be shifted away from the electrode just barely within the diffuse-layer. Fawcett et al.[29−31] also studied the reduction of $Fe(H_2O)_6^{3+}$ ion at three single-crystal gold electrodes and observed that the reduction rate depends on the single crystal used. Large differences in the experimental transfer coefficients at Au(111), Au(100), and Au(110) were attributed to the presence of large double-layer effects. This conclusion was supported by the differences in reduction currents at reconstructed and unreconstructed Au(100) surfaces.[29]

The double-layer effect on the reduction of $Fe(H_2O)_6^{3+}$ ion at four single-crystal gold electrodes has been studied in greater detail in recent work in this laboratory. These results are presented here together with important details regarding the complexity of the $Fe(H_2O)_6^{3+/2+}$ system due to its weak acidity.

Experimental Section

Perchloric acid (Acros Organics, reagent ACS, 70% in water) and ferric perchlorate (Aldrich, low chloride < 0.005%) were of the best quality available from the manufacturer. All solutions were prepared with Nanopure water of maximum resistivity 18 MΩ cm (Barnstead). The glassware was cleaned in boiling 50% nitric acid and washed with Nanopure water before each experiment. All data were obtained using a three-electrode jacketed cell. The working electrodes were single-crystal gold cylinders purchased from Metal Crystals and Oxides Ltd., Cambridge, UK (5N purity oriented to $^1/_2°$ accuracy). The electrode surface was polished with different sizes of alumina powder, the smallest size being 0.05 μm, using the Ecomet3 variable speed polisher, Buehler, Ltd. The electrode surface was then checked under the microscope and electropolished before the flame annealing process. This procedure was followed only with new or aged electrodes, otherwise for a previously pretreated electrode the flame annealing procedure followed by an electropolishing step was usually sufficient to achieve the desired quality of the electrode surface. Before each measurement the electrode was rinsed with Nanopure water, annealed in a butane-air flame and subsequently quenched in the Nanopure water. This procedure was repeated several times. The electrode was then electropolished in perchloric acid solutions by continuous cycling between −0.35 and +1.25V against the 0.05M KCl calomel electrode ($CE_{0.05}$) at a scan rate of 20 mV s^{-1}. The hanging meniscus technique was used to achieve contact of the desired crystal face with the solution in the cell. The effective areas of the electrodes were 0.081 ± 0.001 cm^2 Au(111), 0.099 ± 0.002 cm^2 Au(100), 0.097 ± 0.003 cm^2 Au(110), and 0.103 ± 0.004 cm^2 Au(210). The calomel reference electrode, filled with 0.05 M KCl solution ($CE_{0.05}$), was connected to the cell through a long (15 cm) Luggin capillary filled with perchloric acid in order to minimize contamination of the system with chlorides. A gold counter electrode completed the setup. The experiments were conducted at a constant temperature of 25 °C under an argon atmosphere.

The cleanliness and quality of the electrode surface was verified by cyclic voltammetry by comparing the positions and the shapes of the peaks in the oxide formation region, a final requirement being the coincidence of the potentials of zero charge and the shapes of the capacitance curves in the double-layer region with those reported previously in the literature.[32,33] Cyclic voltammograms (CVs) were obtained using a Princeton Applied Research/PAR 173 potentiostat with a PAR 175 universal programmer employing positive feedback iR compensation. Data were collected either with a PowerLab/4s four-channel analyzer (AD Instruments) or with a Kipp&Zonen BD 91 X−Y recorder. The potentials of zero charge were obtained as an average value of the voltage from scans between −0.5V and +0.5V at a rate 50 mV s^{-1} in both directions. More details concerning the determination of the charge density on the metal and the corresponding double-layer parameters are available in our previous paper.[1] Kinetic parameters were obtained from cyclic voltammograms using the semiintegration analysis described previously.[34−36]

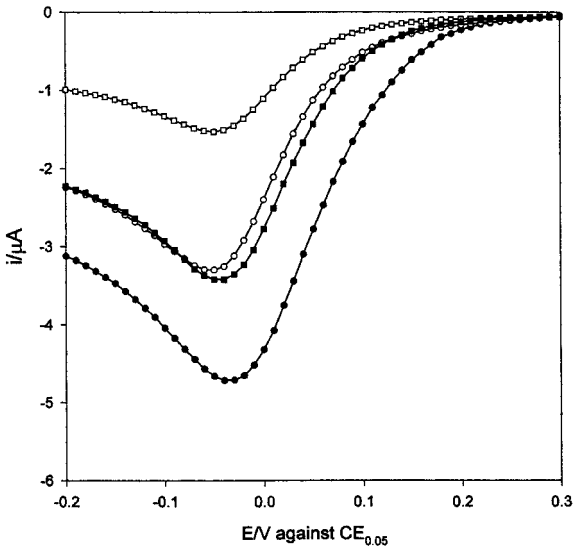

Figure 1. Cyclic voltammograms for the reduction of 10^{-3} M $Fe(ClO_4)_3$ at a Au(210) electrode with T = 25 °C and potential sweep rate of 20 mV s^{-1} with the following concentrations of perchloric acid: 0.01 M (●), 0.05 M (■), 0.1 M (□), and 0.5 M (○).

Results and Discussion

First of all, data for ferric ion reduction obtained in solutions of different perchloric acid concentration at a Au(210) electrode are presented. They illustrate the problems that are encountered with certain systems having complicated solution equilibria.

A series of measurements for the reduction of ferric ion at three different concentrations of perchloric acid were reported earlier at a Au(110) electrode,[28] and contrary to expectations, they showed that the rate constant is only weakly dependent on the perchloric acid concentration. Unfortunately, the situation is not as simple as was originally thought due to the complexity of the equilibria in the bulk of the solution. Complications arise not only directly from the hydrolysis of $Fe(H_2O)_6^{3+}$ ion, but also from the complex formation with perchlorate anion, which, in reality, limits discussion of the double-layer effects for this system to a qualitative level. Ferric ion forms a 1:1 complex with perchlorate. The stability constant of this complex is 14.1 M^{-1} at zero ionic strength[37] and 1.8 M^{-1} at an ionic strength of 0.15 M[38] at T = 25 °C. Additionally, the ferric ion is a weak acid. The dissociation constant for hydrolysis of $Fe(H_2O)_6^{3+}$ to $Fe(H_2O)_5OH^{2+}$ ion is 6.5×10^{-3} at zero ionic strength and 1.3×10^{-3} at an ionic strength of 0.5 M at T = 25 °C.[37] The hydrolysis of $Fe(H_2O)_6^{3+}$ leads further to the formation of $Fe(H_2O)_4(OH)_2^{+}$ and binuclear $Fe_2(OH)_2^{4+}$ ions. However, the contribution of these species can be neglected as each of their bulk concentrations amounts to less than 1% of the total Fe(III) ion concentration in 0.01 M $HClO_4$ solution. Each of their concentrations decreases with increasing acidity of the system.

Figure 1 shows a selected set of CVs obtained for the reduction of 10^{-3} M $Fe(ClO_4)_3$ at Au(210) electrode for four

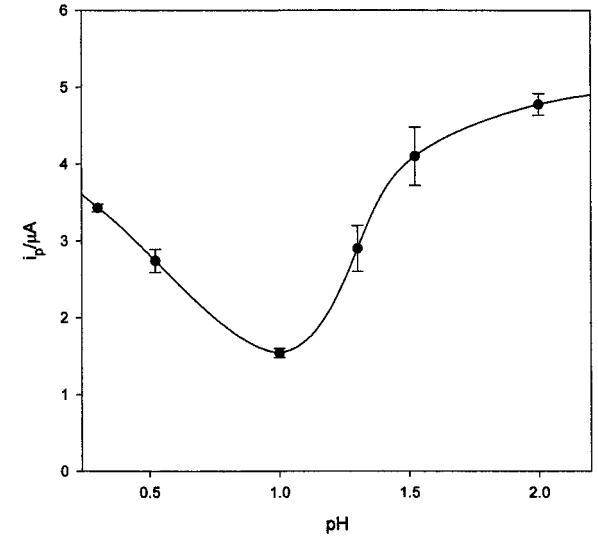

Figure 2. Plot of the peak current as a function of pH from cyclic voltammograms for the reduction of 10^{-3} M $Fe(ClO_4)_3$ in the 0.01 M, 0.03 M, 0.05 M, 0.1 M, 0.3 M, and 0.5 M solutions of perchloric acid. The values shown are averages for at least three measurements. The experimental conditions are the same as in Figure 1.

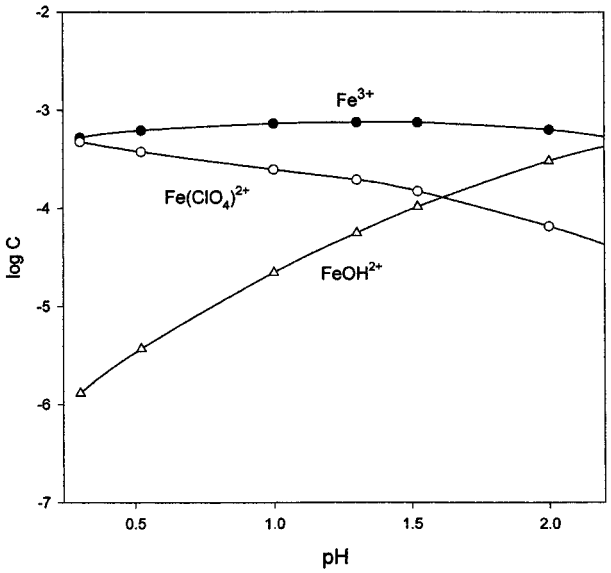

Figure 3. A logarithmic concentration diagram showing the distribution of the three most important Fe(III) species in a solution of 10^{-3} M $Fe(ClO_4)_3$ in perchloric acid.

different concentrations of perchloric acid. Overall, the reduction kinetics were measured at six concentrations of perchloric acid. Figure 2 shows the peak current values as a function of the solution pH. Each point represents an average of at least three measurements. Figure 3 shows the corresponding distribution of ferric species in these solutions. It was obtained using the literature values of the equilibrium constants for the formation of $Fe(H_2O)_6ClO_4^{2+}$ and $Fe(H_2O)_5OH^{2+}$ ions[37,38] that were corrected for the ionic strength of the solutions.

Table 1 contains the calculated concentrations of the Fe(III) species of charge $z = 2+$ and $3+$ in 10^{-3} M $Fe(ClO_4)_3$ as a function of perchloric acid concentration, that is, at varying ionic strength and pH. The species with a charge of $2+$ represent the sum of the concentrations of $Fe(H_2O)_5OH^{2+}$ and $Fe(H_2O)_6(ClO_4)^{2+}$. The fourth column in this table contains the experimental transfer coefficients (α_{ex}) obtained from the CV data after the semiintegration procedure.[34−36] As can be seen the α_{ex} values change moderately with the change in supporting electrolyte concentration. This is similar to observations of Samec[28] reported for the Au(110) electrode. In our case, the α_{ex} values go through a maximum at the same concentration of perchloric acid, at which a minimum is observed in the peak currents (i_p) (Figure 2). The observed changes in the peak current values in Figure 2 are too large to be ignored. Incidentally, they show a trend similar to the changes in the concentration of $z = 2+$ species shown in Table 1. In the last two columns of Table 1, the diffuse-layer potential ϕ^d and the ratio of the concentrations of the $2+$ to $3+$ species at the outer Helmholtz plane (OHP) are given assuming the absence of perchlorate ion adsorption. ϕ^d was estimated from the electrode charge density obtained by integration of the experimental capacitance curves measured in the absence of ferric ions. The values of ϕ^d in Table 1 were calculated using the classical Gouy−Chapman theory and the charge density values at the potential $E - E_z = 0.3$ V. This potential is roughly in the middle of the potential region where kinetic data can be obtained, and corresponds to 0.05 V on the $CE_{0.05}$ reference electrode scale (see Figure 1). The calculated values of ϕ^d were not further corrected for the presence of Fe(III) reactant and product in the double-layer, as this correction is too small to affect the analysis at the level considered here. Values of the diffuse layer potential corrected for the presence of reactant and product at comparable conditions could by found in Figure 6 of Hromadova and Fawcett.[1]

The last column contains the concentration ratio of $z = 2+$ to $z = 3+$ for the Fe(III) species at the OHP, calculated from their bulk concentrations and the ϕ^d values given in Table 1. On the basis of these calculations, the dominant reacting ions at the OHP have a charge of $2+$. This simple calculation explains qualitatively why the changes in the peak currents follow the changes in concentration of the iron species with charge $z = 2+$. However, it does not make the system any simpler because there are still at least two species with charge $z = 2+$, namely $Fe(H_2O)_5OH^{2+}$ and $Fe(H_2O)_6(ClO_4)^{2+}$. In addition, the double-layer calculations in Table 1 are only approximate because there is the possibility that perchlorate is adsorbed at the Au(210) electrode for rational potentials as high as $+0.3$ V. The reduction of ferric ion occurs at far more positive potentials than the reduction of the previously studied $Co(NH_3)_6^{3+}$ ion[1]. There are no literature data directly confirming the adsorption of perchlorate at $E - E_z = 0.3$ V at the Au(210) substrate, but perchlorate ions are adsorbed at the Au(111) electrode at these potentials on the rational scale.[39,40] The perchlorate anions are not specifically adsorbed at the gold electrode when its charge densities are in the range ± 10 μC cm^{-2}. Experimentally obtained charge densities at $E - E_z = 0.3$ V in this paper are ~ 30 μC cm^{-2}. All of these features contribute to the complexity of the system being studied.

The trend in the changes of the peak current with increasing perchloric acid concentration can be reproduced assuming the irreversible reduction of ferric ion and taking into account the measured α_{ex} values and simultaneous diffusion of both $Fe(H_2O)_5OH^{2+}$ and $Fe(H_2O)_6(ClO_4)^{2+}$ species (see Table 2). The experimental values of $c_oD^{1/2}$ were obtained from the equation for the peak current for a totally irreversible system

$$c_oD^{1/2} = i_p/[2.99 \times 10^5(\alpha_{ex})^{1/2}Av^{1/2}] \qquad (1)$$

where i_p is the peak current in A, α_{ex} is the experimental transfer coefficient, A is the electrode area in cm^2, v is the scan rate in V s^{-1}, c_o is the bulk concentration of the reactant in mol cm^{-3}, and D is its diffusion coefficient in cm^2 s^{-1}. The calculated

TABLE 1: Solution Equilibrium, Kinetic and Double-layer Data for the Reduction of 10^{-3} M Fe(III) Ion at a Au(210) Electrode

c($HClO_4$) /M	c($\Sigma Fe(III)^{2+}$) /M[a]	c($\Sigma Fe(III)^{3+}$) /M[b]	α_{ex}[c]	ϕ^d/V [d]	$\left(\frac{\sum Fe(III)^{2+}}{\sum Fe(III)^{3+}}\right)_{\phi^d}^{e}$
0.01	3.69×10^{-4}	6.31×10^{-4}	0.48 ± 0.02	0.20_4	1615
0.03	2.53×10^{-4}	7.47×10^{-4}	0.52 ± 0.02	0.17_9	361
0.05	2.51×10^{-4}	7.49×10^{-4}	0.53 ± 0.02	0.16_9	241
0.1	2.70×10^{-4}	7.30×10^{-4}	0.59 ± 0.02	0.15_5	152
0.3	3.79×10^{-4}	6.21×10^{-4}	0.58 ± 0.02	0.12_8	90
0.5	4.76×10^{-4}	5.24×10^{-4}	0.56 ± 0.02	0.11_6	82

[a] Total concentration of Fe(III) species with a charge of 2+. [b] Total concentration of Fe(III) species with a charge of 3+. [c] Experimental transfer coefficient. [d] Outer Helmholtz plane (OHP) potential estimated from the capacitance curves in the absence of reactant at potential $E - E_z = 0.3$ V assuming the absence of perchlorate ion adsorption. [e] Ratio of the total concentrations of the Fe(III) species of charge 2+ and 3+ estimated at the OHP.

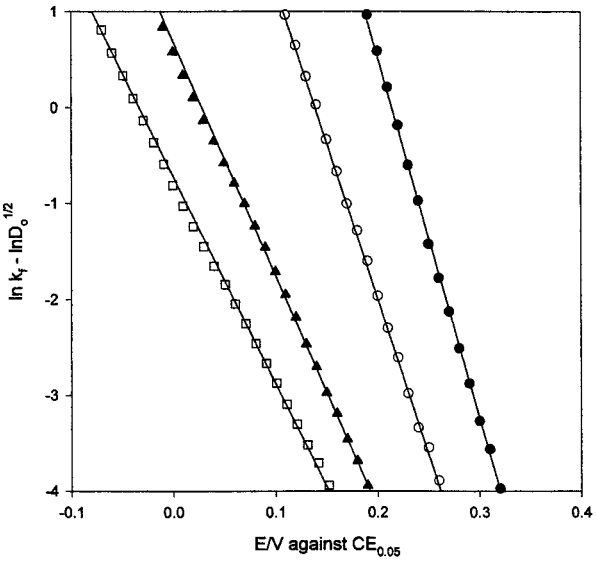

Figure 4. Experimental Tafel plots for the reduction of 2.6×10^{-3} M $Fe(ClO_4)_3$ in 0.1 M perchloric acid, $T = 25$ °C, $\nu = 100$ mV s^{-1} at four single-crystal gold electrodes: Au(111) (●), Au(100) (○), Au(110) (▲), and Au(210) (□).

$c_oD^{1/2}$ values were obtained using the following expression

$$c_oD^{1/2} = c(\sum Fe(III)^{2+})(f_1D_1 + f_2D_2)^{1/2} \qquad (2)$$

where $c(\sum Fe(III)^{2+})$ represents the total concentration of Fe(III) species of charge 2+ (see Table 1), f_1, the mole fraction of $Fe(H_2O)_6(ClO_4)^{2+}$, and f_2, the mole fraction of $Fe(H_2O)_5OH^{2+}$. D_1 and D_2 are the individual diffusion coefficients for these species, respectively. The experimental and calculated values of $c_oD^{1/2}$ are shown in Table 2. Even though the experimental $c_oD^{1/2}$ values are higher by a factor of ~2, they follow the same trend as those calculated using eq 2. The following parameters were used in the determination of the $c_oD^{1/2}$ values: electrode area $A = 0.103$ cm^2, scan rate $\nu = 0.02$ V s^{-1}, diffusion coefficient for $Fe(H_2O)_6(ClO_4)^{2+}$ ion $D_1 = 6.1 \times 10^{-7}$ cm^2 s^{-1}, and for $Fe(H_2O)_5OH^{2+}$ $D_2 = 7.1 \times 10^{-6}$ cm^2 s^{-1}. Several authors[27,28,41] have reported the diffusion coefficient for $Fe(H_2O)_6^{3+}$ ion to be $5.8 \pm 0.4 \times 10^{-6}$ cm^2 s^{-1}. Easteal et al.[42] used conductometric measurements to obtain a limiting value of 6×10^{-6} cm^2 s^{-1} at zero ionic strength. The data of Easteal et al.[42] obtained at different concentrations of ferric perchlorate in perchloric acid were used to estimate the approximate values of the diffusion coefficients for $Fe(H_2O)_6(ClO_4)^{2+}$ and $Fe(H_2O)_5OH^{2+}$ ion quoted above. Samec[28] did not observe these dramatic changes on the diffusion-limited current in his stationary voltammograms. However, UV spectroscopy between 190 and 400 nm indicated the presence of more than one Fe(III) species. It is clear from these experiments that the customary procedure of changing only the perchloric acid concentration is not the best choice in the case of ferric ion, and that rationalization of the kinetic data in Figure 1 is rather difficult.

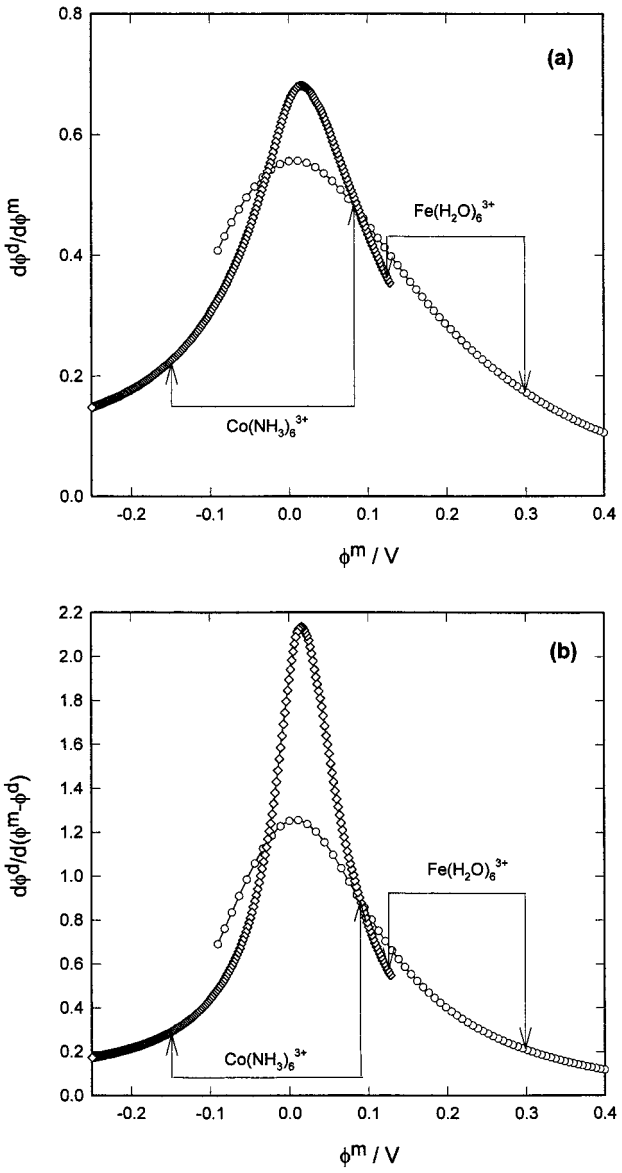

Figure 5. Plots of $d\phi^d/d\phi^m$ (a) and $d\phi^d/d(\phi^m - \phi^d)$ (b) as a function of ϕ^m for Au(210) (circles) and Au(111) (squares) electrode in 0.093 M $HClO_4$ electrolyte. The arrows indicate the ϕ^m values associated with the region of experimentally observed rate constants for the reduction of $Fe(H_2O)_6^{3+}$ and $Co(NH_3)_6^{3+}$ at these electrodes.

Consequently, a simpler strategy was adopted. A solution of

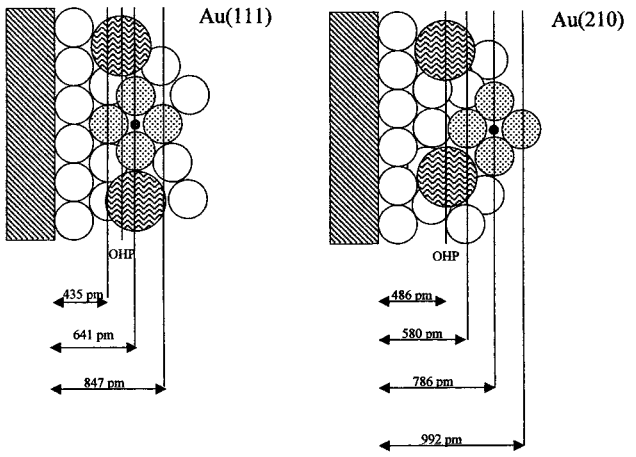

Figure 6. A simplified representation of the electrode/electrolyte interface at positive charge densities in the presence of the $Fe(H_2O)_6(ClO_4)^{2+}$ reactant in the double-layer. Perchlorate anion is represented as a striped sphere and the octahedral hexaaquairon(III) complex has two additional water ligands in the plane perpendicular to the plane of the paper.

2.6×10^{-3} M $Fe(ClO_4)_3$ in 0.1 M perchloric acid was selected to follow the reduction kinetics of the Fe(III) species at four different single-crystal gold electrodes. This choice represents an attempt to minimize the specific adsorption of perchlorate anion and at the same time the presence of a multitude of reducible species. At the composition selected the main reactant in the double-layer region (92%) is the $Fe(H_2O)_6(ClO_4)^{2+}$ ion.

Figure 4 shows the reduction kinetics of Fe(III) ion for this solution composition as a function of the applied potential. The experimental Tafel plots were constructed by semi-integration of the measured CV curves.[34−36] Table 3 contains a summary of the double-layer and kinetic parameters obtained from the analysis of kinetic data in Figure 4. At constant voltage, the reduction rate of Fe(III) ion decreases in the following order: Au(111) > Au(100) > Au(110) > Au(210) (see Figure 4 and Table 3). The same trend was observed previously for the reduction of $Co(NH_3)_6^{3+}$ ion.[1] The experimental transfer coefficients (α_{ex}) were obtained from the slopes of the Tafel plots in Figure 4. They are larger than 0.5 at all four electrodes and decrease from Au(111) to Au(210). This order is opposite to that observed for the reduction of $Co(NH_3)_6^{3+}$ ion at the same electrodes[1] (see Table 4).

The catalytic effect of chloride ions on the reaction rates of both reduction and oxidation of the Fe(III)/(II) couple is well-known.[4,24,28] The maximum level of chloride impurities in the ferric perchlorate solutions used here is certainly lower than 1.3 μM, but there is also a possibility of chloride contamination generated in situ from perchlorate ions in aqueous solutions.[4c] However, careful examination of our data leads to the conclusion that the level of chloride impurities that affects the capacitance and kinetic measurements must be higher than that present in the experiments reported here. Intentional addition of chloride into the present system led eventually to cyclic voltammograms similar to those reported by Hung and Nagy[4c] with a peak to peak separation of about 100 mV between the cathodic and anodic wave. As supporting evidence that the inner sphere pathway is negligible, our experimental transfer coefficient (α_{ex}) for Au(110) electrode can be compared to those obtained by Samec[28] in additionally in-situ purified solutions. Our value of 0.63 ± 0.02 is remarkably close to 0.58 ± 0.02 reported by Samec[28] and also very different from the value of 0.2 that he observed in unpurified solutions or solutions with added sodium chloride (see his Table 2, ref 28). An additional argument in support of the negligible effect of trace chloride impurities on the kinetic parameters obtained in the present study is the comparison of the apparent standard rate constant (k_s^o) reported by Samec[28] at the formal potential of the Fe(III)/Fe(II) couple (1.1×10^{-6} cm s^{-1} in Table 1[28]) to the value extrapolated from Figure 4 of this paper. From the differences in the values of potential of zero charge, we estimated that our reference scale is shifted in the positive direction by 0.29 V. At the potential of 0.39 V against $CE_{0.05}$, which corresponds to the formal potential of the Fe(III)/Fe(II) couple, the highest value of k_s^o available from our experimental measurements in case of the Au(111) electrode is 1.2×10^{-6} cm s^{-1}, assuming an effective diffusion coefficient of 1.14×10^{-6} cm^{-2} s^{-1}. This result is comparable to the values observed by Samec in purified solutions.[28] Therefore, it is safe to assume that the chloride content in the present study was below the level which causes a significant catalytic effect. On the other hand, if the purity of our solutions was not higher than those used in previous studies, it should be noted that the quite different experimental techniques were used in the present experiments. Hung and Nagy[4c] used a potential step technique to obtain the kinetic parameters. Weber et al.[24] and Samec[28] also used a potential step technique at a rotating disk electrode (stationary voltammetry). Our kinetic parameters come from the analysis of cyclic voltammetric curves obtained at scan rates of 20 mV s^{-1} (Figure 1) and 100 mV s^{-1} (Figure 4) and assume irreversible reduction kinetics. The time scale involved in the earlier experiments favors the accumulation of impurities at the electrode surface.

For a simple outer-sphere electron transfer

$$A + e^- \rightarrow B \tag{3}$$

the potential dependence of the reduction rate constant is given by the general expression

$$\ln k_f = \ln k_f^{\,o} - w_A - \alpha(f\phi^m - w_A + w_B) \tag{4}$$

where α is the true transfer coefficient, $f = F/RT$ (38.92 V^{-1} at $t = 25$ °C), w_A and w_B are the work terms (in dimensionless units) associated with bringing the reactant and product to their reaction sites within the double-layer and $k_f^{\,o}$ is the value of the forward rate constant when the rational potential ϕ^m equals to zero. Equation 4 can also be written in terms of the average work w_a of transporting the reactant and product to the reaction site within the double-layer

$$\ln k_f = \ln k_f^{\,o} - w_a - \alpha f\phi^m \tag{5}$$

where

$$w_a = (1 - \alpha)w_A + \alpha w_B \tag{6}$$

For the case of a symmetrical energy barrier α is equal to 0.5 and w_a is the actual average of the work terms w_A and w_B. The experimental transfer coefficient is then expressed in the form

$$\alpha_{ex} = -\frac{1}{f}\frac{\mathrm{d}\ln k_f}{\mathrm{d}\phi^m} = \alpha + \frac{1}{f}\frac{dw_a}{\mathrm{d}\phi^m} \tag{7}$$

and is obtained from the slope of the experimental Tafel plot ln k_f against ϕ^m.

Double-layer effects are normally analyzed using the classical Frumkin approach based on the assumption that the reactant is a point charge z_A located at the OHP. In this case, the experimentally obtained forward rate constant is corrected by

TABLE 2: Comparison of the Experimental and Theoretical $c_oD^{1/2}$ Values[f]

c($HClO_4$) /M	$f(FeOH^{2+})$[a]	$f(FeClO_42+)$[b]	$10^{10}\ c_oD^{1/2}{}_{expt}$/ mol cm^{-2} s$^{-1/2}$ [c]	$10^{10}\ c_oD^{1/2}{}_{calc}$/ mol cm^{-2} s$^{-1/2}$ [d]
0.01	0.82	0.18	15.0[e]	9.0[e]
0.03	0.41	0.59	12.4	4.6
0.05	0.22	0.78	8.5	3.6
0.1	0.08	0.92	4.0	2.9
0.3	0.01	0.99	7.7	3.1
0.5	0	1.00	9.9	3.8

[a] The mole fraction of $Fe(H_2O)_5OH^{2+}$ species. [b] The mole fraction of $Fe(H_2O)_6(ClO_4)^{2+}$ species. [c] $c_oD^{1/2}$ values obtained from the peak currents of the experimental cyclic voltammograms. [d] Theoretical values of $c_oD^{1/2}$ based on the concentration of the reactant of charge 2+. [e] read as 15.0 $\times 10^{-10}$ mol cm^{-2} s$^{-1/2}$. [f] The $c_oD^{1/2}{}_{calc}$ values were obtained using the mole fractions of $Fe(H_2O)_5OH^{2+}$ and $Fe(H_2O)_6(ClO_4)^{2+}$ ions listed below.

TABLE 3: Double-Layer and Kinetic Data for the Reduction of 2.6×10^{-3} M $Fe(ClO_4)_3$ in 0.1 M Perchloric Acid at Single Crystal Gold Electrodes at $T = 25$ °C

electrode	E_z/V	k_f /cm s^{-1}	α_{ex}	$d\phi^d/d\phi^m$	$\alpha_{ex}{}^{calc}$
Au(111)	+0.07	1.8×10^{-3} [a]	0.96 ± 0.02	0.38	0.95[b]
Au(100)	−0.12	1.5×10^{-4}	0.83 ± 0.02	0.30	0.81
Au(110)	−0.17	1.6×10^{-5}	0.63 ± 0.02	0.20	0.64
Au(210)	−0.25	7.0×10^{-6}	0.58 ± 0.02	0.17	0.59

[a] Values taken from Figure 4 at $E = +0.2$V against $CE_{0.05}$ using $D_oeff = 1.14 \times 10^{-6}$ cm^2 s^{-1}. [b] $\alpha_{ex}{}^{calc}$ was obtained using $\alpha_a = 0.3$ in $\alpha_{ex}{}^{calc} = \alpha_a + (2 - \alpha_a)\ d\phi^d/d\phi^m$.

TABLE 4: Double-Layer and Kinetic Data for the Reduction of 5×10^{-4} M $[Co(NH_3)_6](ClO_4)_3$ in 0.0093 M Perchloric Acid at Single Crystal Gold Electrodes at $T = 25$ °C

electrode	E_z/V	k_f /cm s^{-1}	α_{ex}	$d\phi^d/d\phi^m$	$\alpha_{ex}{}^{calc}$
Au(111)	+0.07	1.3×10^{-2} [a]	1.32 ± 0.05	0.28	1.35[b]
Au(100)	−0.12	2.1×10^{-3}	1.38 ± 0.02		
Au(110)	−0.17	3.7×10^{-4}	1.68 ± 0.01	0.65	1.69
Au(210)	−0.25	9.5×10^{-6}	1.74 ± 0.01	0.69	1.72

[a] Values taken from Hromadova and Fawcett[1] at $E = -0.1$ V against $CE_{0.05}$ using $D_o = 8.57 \times 10^{-6}$ cm^2 s^{-1}. [b] $\alpha_{ex}{}^{calc}$ was obtained using $\alpha_a = 1.1$ in $\alpha_{ex}{}^{calc} = \alpha_a + (2 - \alpha_a)\ d\phi^d/d\phi^m$.

adding the term $z_Af\phi^d$ to its logarithm in order to construct the corrected Tafel plot (cTp). Following this traditional approach, eq 5 can be rewritten as

$$\ln k_f + z_Af\phi^d = \ln k_f^{\circ} + (z_A - \alpha)f\phi^d - w_a - \alpha f(\phi^m - \phi^d) \quad (8)$$

where ϕ^d is the potential at the OHP, and $\phi^m - \phi^d$ is the potential drop across the inner layer. The slope of the cTp based on the eq 8 gives then the value of the apparent transfer coefficient α_a

$$\alpha_a = -\frac{1}{f}\frac{d(\ln k_f + z_Af\phi^d)}{d(\phi^m - \phi^d)} = \alpha - (z_A - \alpha)\frac{d\phi^d}{d(\phi^m - \phi^d)} + \frac{1}{f}\frac{dw_a}{d(\phi^m - \phi^d)} \quad (9)$$

Combination of expressions 7 and 9 leads to the relationship between the values of α_{ex} and α_a

$$\alpha_{ex} = \alpha_a + (z_A - \alpha_a)\frac{d\phi^d}{d\phi^m} \quad (10)$$

which is valid regardless of the interpretation of the work terms associated with expressions 7 and 9.

Interpretation of the α_{ex} and α_a values is usually based on the assumption that the reactant and product are point charges being reduced at some distance x^r from the electrode. This distance does not have to coincide with the OHP. Under these assumptions the work terms for the reactant and product are given by the expressions

$$w_A = z_Af\phi^r \quad (11)$$

and

$$w_B = z_Bf\phi^r = (z_A - 1)f\phi^r \quad (12)$$

where z_A and z_B are the point charges on the reactant and product, and ϕ^r is the potential at these points located at a distance x^r from the metal surface.

Defining an adjustable parameter λ that provides an estimate of the position of the reaction site x^r with respect to the position of the OHP x^d and introducing it together with eqs 11 and 12 into the eqs 4 through 9 leads to the following expressions for α_{ex} and α_a[31,43]

$$\alpha_{ex} = \alpha + \lambda(z_A - \alpha) + (z_A - \alpha)(1 - \lambda)\frac{d\phi^d}{d\phi^m} \quad (13)$$

and

$$\alpha_a = \alpha - \lambda(\alpha - z_A) \quad (14)$$

If the reaction site coincides with the OHP, the parameter λ is zero (the potential at the reaction site ϕ^r is equal to ϕ^d) and the α_a is equal to a true transfer coefficient α. When λ is positive or negative, the reaction site is closer or further from the electrode than the OHP plane.

Computation of the position of the reaction site based on the eq 14 can lead to erroneous results, if the reactant is not truly a point charge. It was shown in the previous paper[1] that the reduction of $Co(NH_3)_6^{3+}$ ion can be understood much better when the distribution of charges within the reactant and product is considered.

As a starting point it is useful to analyze the experimental data using eq 10. The experimental α_{ex} values for the reduction of ferric ion are summarized in Table 3. They are compared with the α_{ex} values calculated from eq 10 when α_a is equal to 0.3 and the charge on the reactant is 2+. The $d\phi^d/d\phi^m$ values were obtained from the capacitance curves measured in the absence of ferric ions using the classical Gouy−Chapman−Stern model of the electric double-layer. The agreement between the experimental and calculated α_{ex} values is excellent.

An interesting observation about the reduction of ferric ion at constant ionic strength at different crystallographic orientations of gold is the fact that the α_{ex} values increase when the electrode is changed from Au(210) to Au(111), whereas the opposite trend was observed for the reduction of $Co(NH_3)_6^{3+}$ at these electrodes.[1] Assuming that the term $d\phi^d/d\phi^m$ is the only parameter changing in eq 10 and given that $d\phi^d/d\phi^m$ is approximately constant in the potential range of interest, the

TABLE 5: Comparison of the Double-Layer Parameters for the Reduction of $Co(NH_3)_6^{3+}$ and $Fe(H_2O)_6^{3+}$ Ion in 0.093 M and 0.1 M Perchloric Acid at Au(210) and Au(111) Single Crystal Gold Electrodes at $T = 25^{\circ}C$

	$Co(NH_3)_6^{3+}$					$Fe(H_2O)_6^{3+}$					
electrode	ϕ^m/V	ϕ^d/V	$d\phi^d/d\phi^m$	$d\phi^d/d(\phi^m - \phi^d)$	$\langle z_e \rangle$	ϕ^m/V	ϕ^d/V	$d\phi^d/d\phi^m$	$d\phi^d/d(\phi^m - \phi^d)$	$\langle z_e \rangle$	$\langle z_e \rangle^{calc}$
Au(111)	−0.15	−0.06	+0.23	+0.29	+3.57[a]	+0.12	+0.07	+0.38	+0.60	+1.17[a]	+1.23[b]
Au(210)	+0.08	+0.04	+0.48	+0.93	+2.15	+0.30	+0.11	+0.17	+0.20	+0.50	+0.54

[a] $\langle z_e \rangle$ values based on the experimental $\alpha_a = 1.1$ for $Co(NH_3)_6^{3+}$ and $\alpha_a = 0.3$ for $Fe(H_2O)_6^{3+}$ ion and eq 20. [b] Theoretical $\langle z_e \rangle^{calc}$ values obtained using a geometrical model of the electrode/electrolyte with the distribution of charges taken from the quantum mechanical calculations, see the text and Figure 6.

observed differences in α_{ex} values for $Fe(H_2O)_6^{3+}$ and $Co(NH_3)_6^{3+}$ reduction can be explained by opposite trends in the values of the $d\phi^d/d\phi^m$ terms. As shown in Table 3, the $d\phi^d/d\phi^m$ values increase from Au(210) to Au(111), whereas the opposite trend was observed for the $d\phi^d/d\phi^m$ values in the potential region where the hexaamminecobalt(III) ion is reduced[1] (see Table 4). It should be emphasized that this difference results simply from the fact that the reduction of $Co(NH_3)_6^{3+}$ ion occurs at more negative potentials than the reduction of the $Fe(H_2O)_6^{3+}$ ion at the single-crystal gold electrodes. The values of $d\phi^d/d\phi^m$ obtained from the capacitance data in the potential range, which led to the kinetic results, are shown in Figure 5(a).

On the basis of eq 14, the value of $\alpha_a = 0.3$ and $\lambda = -0.13$ indicate that the reaction site for the reduction of Fe(III) ion is located in the diffuse part of the electrical double-layer. Even though the experimental transfer coefficients are reproduced satisfactorily using eq 10 (see Tables 3 and 4), it has been shown[1] that eq 14 with its λ parameter related to a point charge at the location x^r is entirely inappropriate for rationalization of the α_a value obtained for the reduction of hexaamminecobalt(III) ions. Instead, the observed α_a value was explained by the distribution of charges within the reactant and product.[44−46] To a first approximation, the reactant and product were treated as a set of point charges located at different distances from the electrode. If the charge is distributed at a number of discrete sites within the reactant and product, then

$$w_A = \sum_i z_i f\phi^i \tag{15}$$

and

$$w_B = \sum_j z_j f\phi^j \tag{16}$$

where z_i is the point charge at site i within the reactant, and z_j is the point charge at site j within the product. ϕ^i is the potential at site i and ϕ^j at site j. The α_a value is then expressed by eq 9.

The experimental α_a cefficients were analyzed for $Co(NH_3)_6^{3+}$ and $Fe(H_2O)_6^{3+}$ ions using the experimental $d\phi^d/d(\phi^m - \phi^d)$ values given in Figure 5b. Values at selected potentials, roughly in the middle of the kinetically controlled part of the cyclic voltammograms, are given in Table 5. The $d\phi^d/d(\phi^m - \phi^d)$ values follow the same trend as the previously discussed $d\phi^d/d\phi^m$ terms but are larger in magnitude. Following the treatment proposed previously[5] one defines the effective charge for the reactant

$$z_{Ae} = \frac{\sum_i z_i \phi^i}{\phi^d} \tag{17}$$

and the product

$$z_{Be} = \frac{\sum_j z_j \phi^j}{\phi^d} \tag{18}$$

which is equal to the equivalent point charge located at the OHP. Taking

$$\langle z_e \rangle = (1 - \alpha) z_{Ae} + \alpha z_{Be} \tag{19}$$

the apparent transfer coefficient based on eq 9 is given by

$$\alpha_a = \alpha - (z_A - \alpha - \langle z_e \rangle) \frac{d\phi^d}{d(\phi^m - \phi^d)} \tag{20}$$

Values of $\langle z_e \rangle$ obtained from the experimental α_a and $d\phi^d/d(\phi^m - \phi^d)$ values are given in Table 5. Using eqs 17−19, it is possible to construct a model that satisfies these experimental $\langle z_e \rangle$ values. One such geometrical model is given in Figure 6. It is based on the assumption that the reactant and product form an ion pair with the perchlorate ion. The values of the atomic charges used in the eqs 17 and 18 were taken from the quantum mechanical calculations of Nazmutdinov.[5] The following charges were used for the estimate of $\langle z_e \rangle$ values in Table 5: $z(Fe) = 2.52e$, $z(O) = -1.1e$, $z(H) = 0.59e$ for the $Fe(H_2O)_6^{3+}$ ion and $z(Fe) = 1.84e$, $z(O) = -0.53e$, $z(H) = 0.28e$ for the $Fe(H_2O)_6^{2+}$ ion, where e is the absolute value of the electronic charge. For the sake of simplicity, the charges were localized on the center of the water molecule and the iron atom both of which were modeled as the hard spheres. The center of each sphere gives the position of charge z_i and the potential experienced at this position x^i is expressed as

$$\phi^i = \frac{4}{f} \tanh^{-1}\left\{ \tanh\left(\frac{f\phi^d}{4}\right) \exp[-\kappa(x^i - x^d)] \right\} \tag{21}$$

where κ is the Debye−Hückel reciprocal length. Assuming that the position of OHP is given by the distance of closest approach of the perchlorate anion of radius 226 pm, the OHP is approximately at a distance $x^d \approx 486$ pm from the electrode surface.

Even with this very simplified model of the electrode/electrolyte interface, the calculated $\langle z_e \rangle$ values are in reasonable agreement with their experimental counterparts. Figure 6 suggests that the distance between the reactant and the electrode gets shorter when the electrode is changed from Au(210) to Au(111). The distances of 641 pm and 786 pm between the center of the ion and the electrode surface are in good agreement with theoretical predictions of Smith and Halley[3] for diabatic electron transfer within the $Fe^{3+/2+}$ couple. More detailed calculations based on the concept of the distribution of charges within the reactant and product are given elsewhere.[5]

In conclusion, despite the complexity of this system, the analysis of double-layer effects for Fe(III) system presented here clearly indicates that the reaction site is in the diffuse layer.

Further work in this area requires consideration of reaction couples with smaller charges. An example of such a system is the $[Co(NH_3)_5F]^{2+/1+}$ system. The electrode kinetics of this complex will be discussed in a subsequent paper.

Acknowledgment. The authors are indebted to Dr. Galina A. Tsirlina for very helpful discussions and to Dr. Renat R. Nazmutdinov for carrying out the quantum chemical calculations for the $[Fe(H_2O)_6]^{3+/2+}$ system. This work was supported by a grant from the National Science Foundation (Grant No. CHE-9729314).

References and Notes

(1) Hromadova, M.; Fawcett, W. R. *J. Phys. Chem. A* **2000**, *104*, 4356.
(2) Khan, S. U. M.; Rajt, P.; Bockris, J. O'M. *Elektrokhimiya* **1977**, *13*, 914.
(3) Smith, B. B.; Halley, J. W. *J. Chem. Phys.* **1994**, *101*, 10 915.
(4) Curtiss, L. A.; Halley, J. W.; Hautman, J.; Hung, N. C.; Nagy, Z.; Rhee, Y. J.; Yonco, R. M. *J. Electrochem. Soc.* **1991**, *138*, 2032. (b) Nagy, Z.; Hung, N. C.; Yonco, R. M. *J. Electrochem. Soc.* **1989**, *136*, 895. (c) Hung, N. C.; Nagy, Z. *J. Electrochem. Soc.* **1987**, *134*, 2215.
(5) Fawcett, W. R.; Hromadova, M.; Tsirlina, G. A.; Nazmutdinov, R. R. *J. Electroanal. Chem.*, in press.
(6) Martin, R. L.; Hay, J. P.; Pratt, L. R. *J. Phys. Chem. A* **1998**, *102*, 3565.
(7) Newton, M. D. *J. Phys. Chem.* **1986**, *90*, 3734.
(8) Newton, M. D. *J. Phys. Chem.* **1988**, *92*, 3049.
(9) Friedman, H. L.; Newton, M. D. *J. Electroanal. Chem.* **1986**, *204*, 21.
(10) Kneifel, C. L.; Friedman, H. L.; Newton, M. D. *Z. Naturforsch.* **1989**, *A44*, 385.
(11) Bader, J. S.; Kuharski, R. A.; Chandler, D. *J. Chem. Phys.* **1990**, *93*, 230.
(12) German, E. D.; Kuznetsov, A. M. *Elektrokhimiya* **1990**, *26*, 931.
(13) Bhattacharya-Kodali, I.; Voth, G. A. *J. Phys. Chem.* **1993**, *97*, 11 253.
(14) Rose, D. A.; Benjamin, I. *J. Chem. Phys.* **1994**, *100*, 3545.
(15) Straus, J. B.; Calhoun, A.; Voth, G. A. *J. Chem. Phys.* **1995**, *102*, 529.
(16) Kornyshev, A. A.; Kuznetsov, A. M.; Ulstrup, J. *J. Phys. Chem.* **1994**, *98*, 3832.
(17) Schmickler, W. *Chem. Phys. Lett.* **1995**, *237*, 152.
(18) Pechina, O.; Schmickler, W.; Spohr, E. *J. Electroanal. Chem.* **1995**, *394*, 29.
(19) Benjamin, I. *Chem. Rev.* **1996**, *96*, 1449.
(20) Ohtaki, H.; Radnai T. *Chem. Rev.* **1993**, *93*, 1157.
(21) Herdman, G. J.; Neilson, G. W. *J. Phys. Condens. Matter* **1992**, *4*, 627.
(22) Brunschwig, B. S.; Creutz, C.; Macartney, D. H.; Sham, T. K.; Sutin, N. *Faraday Discuss. Chem. Soc.* **1982**, *74*, 113.
(23) Nagy, Z.; Curtiss, L. A.; Hung, N. C.; Zurawski, D. J.; Yonco, R. M. *J. Electroanal. Chem.* **1992**, *325*, 313.
(24) Weber, J.; Samec, Z.; Mareèek, V. *J. Electroanal. Chem.* **1978**, *89*, 271.
(25) Abdelaal, M. S.; El Miligy, A. A.; Reiners, G.; Lorenz, W. J. *Electrochim. Acta* **1975**, *20*, 507.
(26) Bard, A. J. *Encyclopedia of Electrochemistry of Elements*; Dekker: New York, 1982; Vol. IX, Part A, p 230.
(27) Angell, D. H.; Dickinson, T. *J. Electroanal. Chem.* **1972**, *35*, 55.
(28) Samec, Z. *J. Electrochem. Soc.* **1999**, *146*, 3349.
(29) Fawcett, W. R.; Fedurco, M.; Kováčová, Z. *J. Electrochem. Soc.* **1994**, *141*, L30.
(30) Fawcett, W. R. *Electrochim. Acta* **1997**, *42*, 833.
(31) Fawcett, W. R. *Electrocatalysis*; Lipkowski, J., Ross, P. N., Eds.; Wiley-VCH: New York, 1998; p 323.
(32) Hamelin, A. *J. Electroanal. Chem.* **1996**, *407*, 1.
(33) Hamelin, A.; Martins, A. M. *J. Electroanal. Chem.* **1996**, *407*, 13.
(34) Imbeaux, J. C.; Savéant, J. M. *J. Electroanal. Chem.* **1973**, *44*, 169.
(35) Savéant, J. M.; Tessier, D. *J. Electroanal. Chem.* **1975**, *65*, 57.
(36) Oldham, K. B. *J. Electroanal. Chem.* **1986**, *208*, 1.
(37) Smith, R. M.; Martell, A. E. *Critical Stability Constants*; Plenum Press: New York, 1976; Vol. 4: Inorganic Complexes, p 114.
(38) Fordham, A. W. *Aust. J. Chem.* **1969**, *22*, 1111.
(39) Calvente, J. J.; Marinković, N. S.; Kováčová, Z.; Fawcett, W. R. *J. Electroanal. Chem.* **1997**, *421*, 49.
(40) Ataka, K.; Yotsuyanagi, T.; Osawa, M. *J. Phys. Chem.* **1996**, *100*, 10 664.
(41) Benari, M. D.; Hefter, G. T. *Electrochim. Acta* **1991**, *36*, 471.
(42) Easteal, A. J.; Price, W. E.; Woolf, L. A. *J. Phys. Chem.* **1989**, *93*, 7517.
(43) Fawcett, W. R. *Can. J. Chem.* **1981**, *59*, 1844.
(44) Nazmutdinov, R. R.; Tsirlina, G. A.; Kharkats, Y. I.; Petrii, O. A.; Probst, M. *J. Phys. Chem. B* **1998**, *102*, 677.
(45) Tsirlina, G. A.; Kharkats, Y. I.; Nazmutdinov, R. R.; Petrii, O. A. *Elektrokhimiya* **1999**, *35*, 23.
(46) Khrushcheva, M. L.; Tsirlina, G. A.; Petrii, O. A. *Elektrokhimiya* **1998**, *34*, 355.